Research Article Open Access

Sebastian Różowicz*

Use of the mathematical model of the ignition system to analyze the spark discharge, including the destruction of spark plug electrodes

https://doi.org/10.1515/phys-2018-0011
Received October 31, 2017; accepted November 30, 2017

Abstract: The paper presents the results of analytical and experimental studies concerning the influence of different kinds of fuel additives on the quality of the spark discharge for different configurations of the ignition system. The wear of the spark plug electrode and the value of spark discharge were determined for various impurities and configurations of the air-fuel mixture.

Keywords: ignition system, spark plugs, fuel mixture impurities, microstructure, laser welding, refractory materials

PACS: 07.05.Bx, 07.05.Tp, 01.50.Pa , 02.60.Cb

1 Introduction

The dynamic development of the automotive industry in recent decades has been linked to the continuous improvement of the components of internal combustion engines. Consequently, increased reliability and better environmental performance have been achieved. One of the components that considerably influenced those two factors is the ignition system [1, 2, 5, 9, 11–14]. The purpose of the ignition system is to provide the electrical spark to ignite air fuel mixture in the cylinder at the appropriate time and with the required spark discharge energy [1, 3, 4, 6]. It is vital that the electrical charge provided by the ignition system to the plug be of high frequency, high stability and sufficient duration. All the properties of the spark discharge significantly affect the quality of the combustion process of the fuel-air mixture in the engine cylinder, and therefore the toxicity of the exhaust gas. In addition, to prevent the detonation in the fuel, additives are usually used. Some fuel (mixture) combustion products may accumulate on the power supply components (plug insulators) or in the combustion chamber of the engine, thereby reducing emission or hindering the ignition of the mixture, which results in the increased toxicity of the exhaust gas. The increased degradation of the ignition system components (the spark plug) affects the spark energy value and leads to the increased wear of the spark plug electrode. The use of worn spark plug in the increased temperature of the combustion chamber can result in uneven engine operation, loss of power and increased fuel consumption. The dynamics of the phenomena in the ignition system together with the influence of external factors make the analysis a difficult research problem. Many scientists around the world carry out research into optimum operation of ignition system. However, the results of the simulation tests differ from those obtained experimentally.

In the paper an attempt is made to analyse the operation of the ignition system by means of digital simulation and subsequent verification of the results obtained on a real object. Both the spark energy value for different levels of impurities in the air-fuel mixture and the wear of the plug electrode were determined.

2 Toxic components in the exhaust gases

In the exhaust gas the level of CO, C_mH_n, NO_x and soot levels in diesel engines should be subject to control. Carbon monoxide and hydrocarbons are produced as a result of the incomplete combustion process, where CO depends on the coefficient λ. Nitrogen oxides are the natural chemical products of the combustion reaction. The effect of the composition of the mixture on the toxic constituents of the exhaust gas is shown in Figure 1.

There are several ways to reduce the toxicity of exhaust by acting on the composition of the mixture. One of the

***Corresponding Author: Sebastian Różowicz:** Kielce University of Technology, Department of Electrical Engineering, Automatics and Computer Science, Kielce, al. Tysiąclecia Państwa Polskiego 7, Poland, E-mail: s.rozowicz@tu.kielce.pl

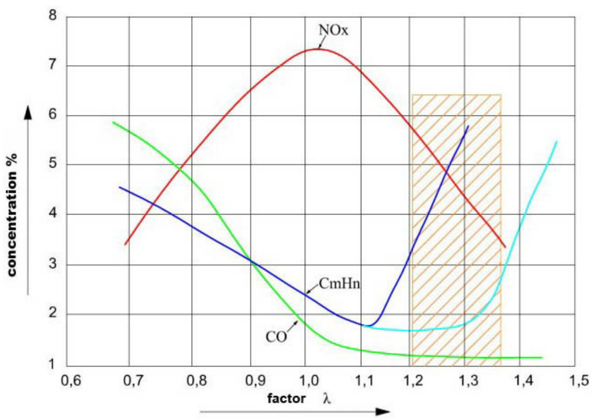

Figure 1: The content of toxic components in the exhaust gas as a function of the composition of the mixture [8]

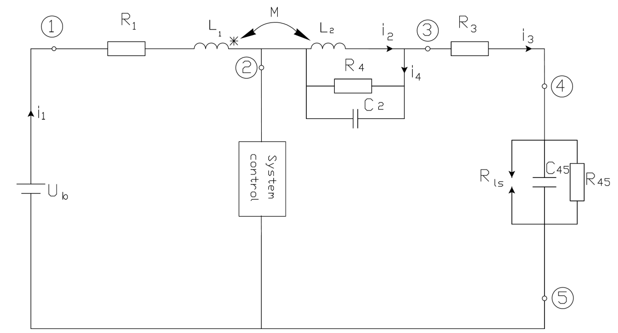

Figure 2: Model of the ignition system for the simulation studies. U_b – battery voltage, R_1 – resistance of the ignition coil primary winding, L_1 – inductance of the ignition coil primary winding, L_2 – inductance of the ignition coil secondary winding, R_2 – resistance of the ignition coil secondary winding, R_4 – resistance representing the losses in the coil core, R_3 – radioelectrical interference resistance, R_{45} – flow resistance of the spark plug, R_{ls} – discharge resistance, C_2 – self-capacity of the coil, C_{45} – selfcapacity of the spark plug, M – coupling [1, 2]

methods is to feed the engine with a lean mixture (λ = 1,2 ÷ 1,3). This reduces the content of nitrogen oxides NO_x, but then at the same time the level of hydrocarbons C_mH_n raises. Requirements for the precise dosage of fuel are very high, because the mix is depleted to the flammable limit. This method of NO_x reduction has proved to be unfavorable, since the engine develops lower power, while wear of spark plugs and simultaneously fuel consumption are increased. When the engine power supply is rich (λ = 0.7 - 0.55), the content of NO_x is also relatively low. The increased emission of C_mH_n and CO can be reduced by using an afterburner in the exhaust system. The disadvantage of this solution is the increased fuel consumption, up to 30%. The study showed that the best settlement is to feed the engine with stoichiometric mixture (λ = 1). On the other hand, when it is fed with the rich mixture, low presence of CO and NO_x is reduced to free N_2. Then the afterburner does not cause reduction of nitrogen oxides, because the excess oxygen, and too small amount of CO prevent the reduction of NO_x to N_2 [8, 11–15].

3 Model of the ignition system

Ignition systems accumulating energy in inductance are more commonly used than those accumulating energy in capacitance [1–3]. In Figure 2 a diagram of ignition system used to build a mathematical model is shown.

The equivalent circuit of the ignition system presented in Figure 2 is described by equations (1) for two states of the control block.

$$U_B - i_1R_1 - L_1\frac{di_1}{dt} + M\frac{di_2}{dt} = 0,$$
$$L_2\frac{di_2}{dt} - M\frac{di_1}{dt} + i_2R_2 + i_3R_3 + u_{C45} = 0,$$

$$\begin{aligned} u_{C2} &= L_2\frac{di_2}{dt} - M\frac{di_1}{dt} + i_2R_2, \\ u_{C2} &= i_{R4}R_4, \quad i_3 = i_2 + i_{R4} + i_{C2} \\ i_3 &= i_{R45} + i_{C45}, \quad u_{C45} = i_{R45}R_{45} \\ i_{C2} &= C_2\frac{du_{C2}}{dt}, \quad i_{C45} = C_{45}\frac{du_{C45}}{dt} \end{aligned} \tag{1}$$

By introducing state variables: $x_1 = i_1$, $x_2 = i_2$, $x_3 = u_{C2}$, $x_4 = u_{C45}$ to the equation (1):

$$\begin{aligned} &U_B - x_1R_1 - L_1\frac{dx_1}{dt} + M\frac{dx_2}{dt} = 0, \\ &L_2\frac{dx_2}{dt} - M\frac{dx_1}{dt} + x_2R_2 + R_3\frac{x_4}{R_{45}} + R_3C_{45}\frac{dx_4}{dt} + x_4 = 0, \\ &x_3 = L_2\frac{dx_2}{dt} - M\frac{dx_1}{dt} + x_2R_2 \\ &\frac{x_4}{R_{45}} + C_{45}\frac{dx_4}{dt} = x_2 + \frac{x_3}{R_4} + C_2\frac{dx_3}{dt} \end{aligned} \tag{2}$$

Transforming the system of equations (2), we obtain:

$$\begin{aligned} \frac{dx_1}{dt} &= A_1x_1 + B_1x_2 + C_1x_3 + D_1U_B \\ \frac{dx_2}{dt} &= A_2x_1 + B_2x_2 + C_2x_3 + D_2U_B \\ \frac{dx_3}{dt} &= A_3x_1 + B_3x_2 + C_3x_3 + E_3x_3 + D_3U_B \\ \frac{dx_4}{dt} &= A_4x_1 + B_4x_2 + C_4x_3 + E_4x_4 + D_4U_B \end{aligned} \tag{3}$$

where the parameters are determined using the following relationships:

$$A_1 = \frac{R_1}{\left(\frac{M^2}{L_2} - L_1\right)},$$

$$B_1 = \frac{MR_2}{L_2\left(\frac{M^2}{L_2} - L_1\right)},$$

$$
\begin{aligned}
C_1 &= -\frac{M}{L_2\left(\frac{M^2}{L_2}-L_1\right)},\\
D_1 &= -\frac{1}{\left(\frac{M^2}{L_2}-L_1\right)},\\
A_2 &= \frac{-MR_1}{L_1\left(L_2-\frac{M^2}{L_1}\right)},\\
B_2 &= \frac{-R_2}{\left(L_2-\frac{M^2}{L_1}\right)},\\
C_2 &= \frac{1}{\left(L_2-\frac{M^2}{L_1}\right)},\\
D_2 &= \frac{M}{L_1\left(L_2-\frac{M^2}{L_1}\right)},\\
A_3 &= \frac{C_{45}A_4}{C_2}, B_3 = \left(\frac{C_{45}B_4}{C_2}-\frac{1}{C_2}\right), C_3 = \left(\frac{C_{45}C_4}{C_2}-\frac{1}{C_2}\right),\\
D_3 &= \frac{C_{45}}{C_2}D_4U_B, E_3 = \left(\frac{1}{C_2R_{45}}+\frac{C_{45}E_4}{C_2}\right),\\
A_4 &= \left(\frac{MA_1}{2R_3C_{45}-\frac{L_2A_2}{2R_3C_{45}}}\right),\\
B_4 &= \left(\frac{MB_1}{2R_3C_{45}}-\frac{L_2B_2}{2R_3C_{45}}+\frac{R_2}{2R_3C_{45}}\right),\\
C_4 &= \left(\frac{MC_1}{2R_3C_{45}}-\frac{L_2C_2}{2R_3C_{45}}\right),\\
D_4 &= \frac{-L_2D_2}{2R_3C_{45}}, E_4 = -\left(\frac{R_3}{2R_3C_{45}R_{45}}+\frac{1}{2R_3C_{45}}\right)
\end{aligned}
\tag{4}
$$

The solution to Equation (3) has the form:

$$
x = \begin{bmatrix} x_1\\ x_2\\ x_3\\ x_4 \end{bmatrix}, A = \begin{bmatrix} A_1 & B_1 & C_1 & 0\\ A_2 & B_2 & C_2 & 0\\ A_3 & B_3 & C_3 & E_3\\ A_4 & B_4 & C_4 & E_4 \end{bmatrix}, B = U_B\begin{bmatrix} D_1\\ D_2\\ D_3\\ D_4 \end{bmatrix} \tag{5}
$$

At the first switch-on, the initial conditions are zero and Eq. (5) assumes the form:

$$
\begin{aligned}
\frac{d}{dt}x &= Ax + B,\\
x &= \mathrm{e}^{At}x_0 + \int_0^t \mathrm{e}^{A(t-\tau)}Bd\tau,\\
x &= \int_0^t \mathrm{e}^{A(t-\tau)}Bd\tau
\end{aligned}
\tag{6}
$$

The solution of equations for the control block (Figure 2) in the open state was obtained by using the state variable method.

The next stage of the calculation (7) refers to the operation of the system with the closed-loop control block where the initial conditions, i.e., the final conditions of the previous state (1), have to be calculated from the control block formula in the contact state for the time equal to the time of contact.

$$
\begin{aligned}
&U_B - i_3R_1 - L_1\frac{di_3}{dt} + M\frac{di_2}{dt} - L_2\frac{di_2}{dt} + M\frac{di_3}{dt} - i_3R_3 - u_{C45} = 0,\\
&u_{C2} = L_2\frac{di_2}{dt} - M\frac{di_3}{dt} + i_2R_2,\\
&u_{C2} = i_{R4}R_4,\quad i_3 = i_2 + i_{R4} + i_{C2},\\
&i_3 = i_{R45} + i_{C45},\quad u_{C45} = i_{R45}R_{45},\\
&i_{C2} = C_2\frac{du_{C2}}{dt},\quad i_{C45} = C_{45}\frac{du_{C45}}{dt}
\end{aligned}
\tag{7}
$$

In this case, the unknowns are: i_2, i_3, i_{R4}, i_{C2}, i_{R45}, i_{C45}, u_{C2}, and u_{C45}.

By introducing state variables: $x_1 = i_2$, $x_2 = i_3$, $x_3 = u_{C2}$, $x_4 = u_{C45}$ to the equation (7):

$$
\begin{aligned}
&U_B - x_2(R_1+R_3) + (M-L_1)\frac{dx_2}{dt} + (M-L_2)\frac{dx_1}{dt} - x_4 = 0\\
&x_3 = L_2\frac{dx_1}{dt} - M\frac{dx_2}{dt} + x_1R_2 \to \frac{dx_2}{dt} = \frac{L_2}{M}\frac{dx_1}{dt} + x_1\frac{R_2}{M} - \frac{1}{M}x_3\\
&x_2 = x_1 + \frac{x_3}{R_4} + C_2\frac{x_3}{dt} \to C_2\frac{x_3}{dt} = -x_1 + x_2 - \frac{x_3}{R_4}\\
&x_2 = \frac{x_4}{R_{45}} + C_{45}\frac{dx_4}{dt} \to C_{45}\frac{dx_4}{dt} = x_2 - \frac{x_4}{R_{45}}
\end{aligned}
\tag{8}
$$

Transforming the system of equations (8), we obtain:

$$
\begin{aligned}
\frac{dx_1}{dt} &= a_1x_1 + b_1x_2 + c_1x_3 + d_1x_4 + e_1U_B\\
\frac{dx_2}{dt} &= a_2x_1 + b_2x_2 + c_2x_3 + d_2x_4 + e_2U_B\\
\frac{dx_3}{dt} &= a_3x_1 + b_3x_2 + c_3x_3\\
\frac{dx_4}{dt} &= b_4x_2 + d_4x_4
\end{aligned}
\tag{9}
$$

For the system of equations (9) the parameters $a_1 \ldots d_4$ are defined by the relationships:

$$
\begin{aligned}
a_1 &= -\frac{R_2(M-L_1)}{[L_2(M-L_1)+M(M-L_2)]},\\
b_1 &= \frac{M(R_1+R_3)}{[L_2(M-L_1)+M(M-L_2)]},\\
c_1 &= \frac{(M-L_1)}{[L_2(M-L_1)+M(M-L_2)]},\\
d_1 &= \frac{M}{[L_2(M-L_1)+M(M-L_2)]},\\
e_1 &= -d_1,\\
a_2 &= \frac{a_1L_2+R_2}{M}, b_2 = \frac{b_1L_2}{M}, c_2 = \frac{c_1L_2-1}{M}\\
d_2 &= \frac{d_1L_2}{M}, e_2 = -\frac{e_1L_2}{M}\\
a_3 &= -\frac{1}{C_2}, b_3 = \frac{1}{C_2}, c_3 = -\frac{1}{C_2R_4},\\
b_4 &= \frac{1}{C_{45}}, d_4 = -\frac{1}{C_{45}R_{45}}
\end{aligned}
\tag{10}
$$

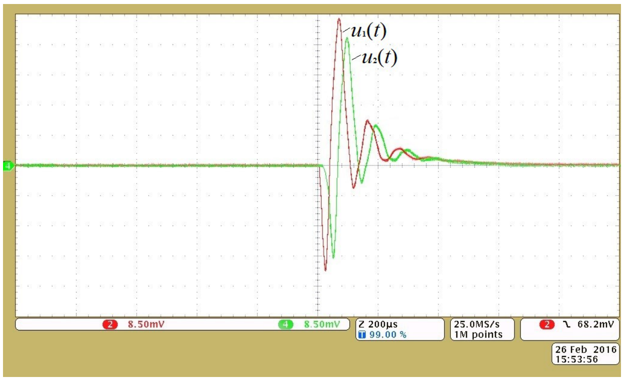

Figure 3: Secondary voltage for new spark plug $u_1(t)$ and voltage $u_2(t)$ for spark plug after 30 hours of working with contaminated fuel

The solution to Equation (9) has the form:

$$x = \begin{bmatrix} x_1 \\ x_2 \\ x_3 \\ x_4 \end{bmatrix}, A = \begin{bmatrix} a_1 & b_1 & c_1 & d_1 \\ a_2 & b_2 & c_2 & d_2 \\ a_3 & b_3 & c_3 & 0 \\ 0 & b_4 & 0 & d_4 \end{bmatrix}, B = U_B \begin{bmatrix} e_1 \\ e_2 \\ 0 \\ 0 \end{bmatrix} \tag{11}$$

Eq. (9) assumes the form:

$$\frac{d}{dt}x = Ax + B,$$
$$x = \mathrm{e}^{At}x_0 + \int_0^t \mathrm{e}^{A(t-\tau)}B d\tau \tag{12}$$

x_0 – initial conditions, or final conditions from the previous state, to be calculated from the formulae for the control block in the contact state for the time equal to the time of contact [2].

The time t will be counted from the moment the block is no longer in the contact state.

The results of the computer simulation shown in Figure 3 show the difference in the voltage waveforms $u_1(t)$ and $u_2(t)$. It is evident that the response of $u_2(t)$ (the output voltage to the new spark plug) is different from the response of the spark plug working for 40 hours with contaminated fuel.

It is worth getting to know even the outline of the waveforms that arise as a result of the load of the ignition wire by components such as the spark plug. We often see the effects of reflections on the ends of cables and multiple overlapping of the reflected waves. It can be assumed that such a match will have a significant impact on the spark discharge and consequently the energy, the reliability of the ignition or, of such importance in the present day, the toxicity of exhaust gases. In summary, it seems that the more appropriate model of the ignition system should

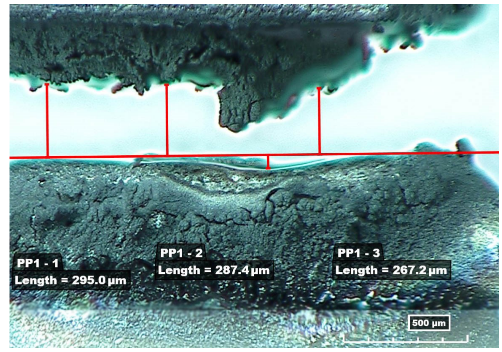

(a) spark plug NGK WR3 after 10 hour of operation at 500°C- capacitive

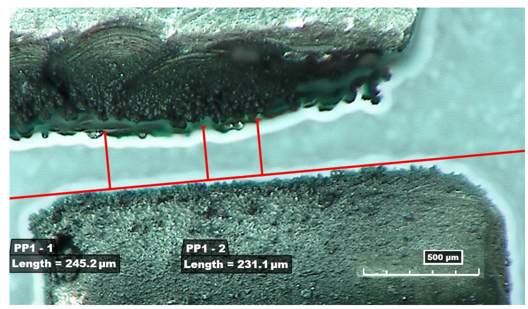

(b) spark plug NGK WR3 after 10 hour operation at 500°C - induction

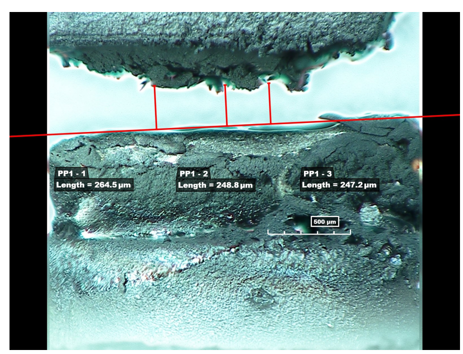

(c) spark plug NGK WR3 after 30 hour operation at 500°C- capacitive

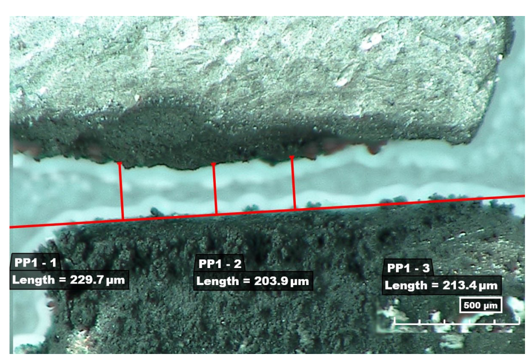

(d) spark plug NGK WR3 after 30 hour operation at 500°C - induction

Figure 4: The image of the gap between electrodes

be the model (being developed by the authors of this paper), which takes into account, in addition, the shape of the spark plug electrodes and the description of the ignition cable as a distributed system.

4 Results of studies

4.1 The effect of fuel impurities on the wear of spark plug electrodes

In both types of ignition systems, one-electrode NGK spark plugs were used. The tests were carried out at combustion temperature of the fuel-air mixture of 500° C. First assessment of the spark plug wear was made after 10 hours of service (Figure 4a, 4b), and the next after 30 hours (Figure 4c, 4d). In all experiments the air-fuel mixture containing impurities was used.

The analysis of the wear of emission surfaces of electrodes was conducted using HIROX KH-8700 electron scanning microscope.

4.2 Determination of spark discharge energy for different types of electrodes

For an 30 hour operation of spark plugs at 500°C for spark plugs NGK discharge energy for capacitor discharge system, calculated on the basis of the results presented in Figure 5a and 5b, amounts to 32.6 mJ.

5 Conclusion

Very good results in NO_x reduction can be achieved by using spark plugs with increased hardness of the electrodes by surfacing. As it is shown by simulated studies, (Figure 5a and 5b), the most advantageous fuel-air mixture for the internal combustion engine is a stoichiometric mixture ($\lambda = 1$).

The results of the study indicate that the energy of the spark discharge after 30 hours of operation has decreased by about 10% compared to the initial state.

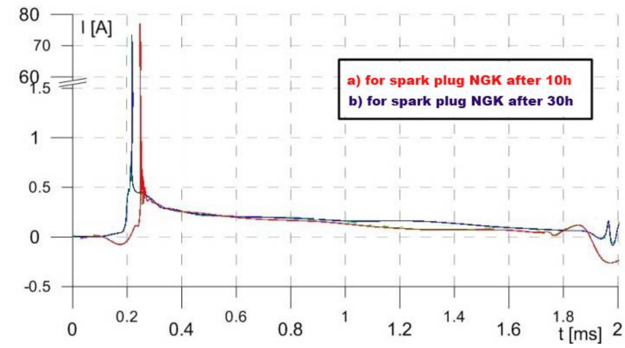

(a)

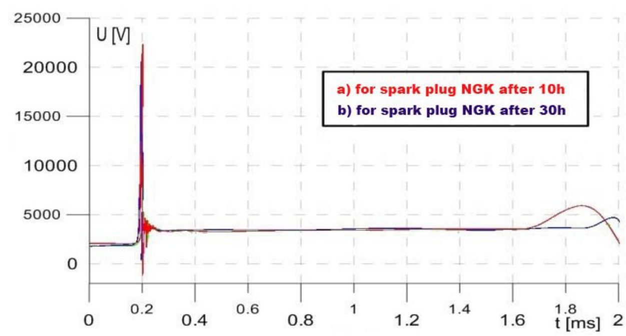

(b)

Figure 5: (a) Current for 10 hour and 30 hour operation of spark plugs at 500°C; (b) Voltage for 10 hour and 30 hour operation of spark plugs at 500°C
Calculated energy is: E = 32.6 mJ

References

[1] Różowicz S., Tofil S., Influence of fuel impurities on the consumption of electrodes in spark plugs, 18th International Symposium on Electromagnetic Fields in Mechatronics, Electrical and Electronic Engineering, 14-16 September 2017, Lodz, Poland.

[2] Różowicz S., Tofil Sz., The influence of impurities on the operation of selected fuel ignition systems in combustion engines, Archives of Electrical Engineering, 2016, 65(2), 349-360, DOI: 10.1515/aee-2016-0026.

[3] Robinet C., Andrzejewski J., Higelin P., Cycle-to-Cycle Variation Study of an SI Engine Fired by Spark Plug and a Non Conventional Device, SAE, 1997, 972986

[4] Zawadzki A., Różowicz S., Application of input - State of the system transformation for linearization of some nonlinear generators, Int. J. Contr., Automation and Systems, DOI: 10.1007/s12555-014-0026-3.

[5] Zawadzki A., Różowicz S., Application of input-state of the system transformation for linearization of selected electrical circuits, J. Electr. Eng., 2016, 67, 3, 199-205, DOI: 10.1515/jee-2016-0028.

[6] Alger T., Mangold B., Mehta D., Roberts C., The effect of Sparkplug Design on Initial Flame Kernel Development and Sparkplug Performance, SAE, 2006.

[7] Antoszewski B., Tofil Sz., The laser welding of iridium-platinum tips to spark plug electrodes, Proc. SPIE 10159, Laser Technology 2016: Progress and Applications of Lasers, 2016, 10159.

[8] Różowicz S., The effect of parameter change of ignition system primary side R,L and C elements on the value of spark discharge energy (in Polish), Przegląd Elektrotechniczny, ISSN 0033-2097,

2016, 5, 92
[9] Różowicz S., Analysis of the effect of the ignition system construction and parameters on the value of the discharge energy, PhD dissertation (in Polish), PŚK 2012
[10] Stone C., Brown A., Beckwith P., Cycle-by-cycle variations in spark ignition engine combustion – part II: modeling of flame kernel displacements as a cause of cycle-by-cycle variations, SAE, 1996, 960613
[11] Robinet C., Andrzejewski J., Higelin P., Cycle-to-cycle variation study of an si engine fired by spark plug and a non-conventional device, SAE, 1997, 972986
[12] Hunicz J., Wac E., Kabała J., Comparative study of new spark plug designs, operation and reliability, Operation and Reliability (in Polish) 2006, 3
[13] Herweg R., Ziegler G.F.W., Flame kernel formation in a sparkignition engine, In: International sym-posium COMODIA 90, 1990, 173-178.
[14] Lee K., Kim K., Influence of initial combustion in SI engine on following combustion stage and cycle-by-cycle variations in combustion process, Int. J. Automot. Technol., 2001, 2(1), 25-31.
[15] Lee Y., Boehler J., Flame kernel development and its effects on engine performance with various spark plug electrode configurations, SAE 2005, 1, 1133